

Overview of RFX fusion science program

P. Martin 1), J. Adamek 2), P. Agostinetti 1), M. Agostini 1), A. Alfier 1), C. Angioni 3), V. Antoni 1), L. Apolloni 1), F. Auriemma 1), O. Barana 1), S. Barison 4), M. Baruzzo 1), P. Bettini 1), M. Boldrin 1), T. Bolzonella 1), D. Bonfiglio 1), F. Bonomo 1), A. H. Boozer 5) 6), M. Brombin 1), J. Brotankova 2), A. Buffa 1), A. Canton 1), S. Cappello 1), L. Carraro 1), R. Cavazzana 1), M. Cavinato 1) 23), L. Chacon 7), G. Chitarin 1), W. A. Cooper 8), S. Dal Bello 1), M. Dalla Palma 1), R. Delogu 1), A. De Lorenzi 1), G. De Masi 1), J. Q. Dong 9), M. Drevlak 10), D. F. Escande 11), F. Fantini 1), A. Fassina 1), F. Fellin 1), A. Ferro 1), S. Fiameni 4), A. Fiorentin 1), P. Franz 1), E. Gaio 1), X. Garbet 12), E. Gazza 1), L. Giudicotti 1), F. Gnesotto 1), M. Gobbin 1), L. Grandi 1), S. C. Guo 1), S. P. Hirshman 7), S. Ide 13), V. Igochine 3), Y. In 14), P. Innocente 1), S. F. Liu 15), Y. Q. Liu 16), D. López Bruna 17), R. Lorenzini 1), A. Luchetta 1), G. Manduchi 1), D. K. Mansfield 6), G. Marchiori 1), D. Marcuzzi 1), L. Marrelli 1), S. Martini 1), G. Matsunaga 13), E. Martines 1), G. Mazzitelli 18), K. McCollam 19), S. Menmuir 1), F. Milani 1), B. Momo 1), M. Moresco 1), S. Munaretto 1), L. Novello 1), M. Okabayashi 6), S. Ortolani 1), R. Paccagnella 1), R. Pasqualotto 1), M. Pavei 1), G. V. Perverezhev 3), S. Peruzzo 1), R. Piovan 1), P. Piovesan 1), L. Piron 1), A. Pizzimenti 1), N. Pomaro 1), N. Pomphrey 6), I. Predebon 1), M. E. Puiatti 1), V. Rigato 1), A. Rizzolo 1), G. Rostagni 1), G. Rubinacci 20), A. Ruzzon 1), R. Sanchez 7) 21), J. S. Sarff 19), F. Sattin 1), A. Scaggion 1), P. Scarin 1), G. Serianni 1), P. Sonato 1), E. Spada 1), A. Soppelsa 1), S. Spagnolo 1), M. Spolaore 1), D. A. Spong 7), G. Spizzo 1), M. Takechi 13), C. Taliercio 1), D. Terranova 1), V. Toigo 1), M. Valisa 1), M. Veranda 1), N. Vianello 1), F. Villone 22), Z. Wang 1), R. B. White 6), D. Yadikin 3), P. Zaccaria 1), A. Zamengo 1), P. Zanca 1), B. Zaniol 1), L. Zanutto 1), E. Zilli 1), G. Zollino 1), M. Zuin 1)

- 1) Consorzio RFX, Associazione EURATOM-ENEA sulla Fusione, 35137 Padova, Italy
- 2) Institute of Plasma Physics, Association EURATOM-IPP.CR, Prague, Czech Republic
- 3) Max-Planck-Institut für Plasmaphysik, EURATOM Association, 85748 Garching, Germany
- 4) CNR-IENI, Corso Stati Uniti 4, 35127 Padova, Italy
- 5) Dept. of Applied Physics and Applied Mathematics, Columbia University, New York, NY, USA
- 6) Princeton Plasma Physics Laboratory, Princeton, NJ, USA
- 7) ORNL Fusion Energy Division, Oak Ridge, TN, USA
- 8) EPFL, Association EURATOM-Confederation Suisse, Centre de Recherches en Physique des Plasmas, Lausanne, Switzerland
- 9) Institute for Fusion Theory and Simulation, Zhejiang Univ, Hangzhou, Southwestern Institute of Physics, Chengdu, People's Republic of China
- 10) Max-Planck-Institut für Plasmaphysik, EURATOM Association, Greifswald, Germany
- 11) UMR 6633 CNRS-Université de Provence, Marseille, France
- 12) CEA, IRFM, F-13108 Saint Paul Lez Durance, France
- 13) Japan Atomic Energy Agency, Naka, Ibaraki 311-0193 Japan
- 14) FAR-TECH, Inc., 3550 General Atomics Ct, San Diego, CA 92121, USA
- 15) Department of Physics, Nankai University, Tianjin 300071, People's Republic of China
- 16) EURATOM/CCFE Fusion Association, Culham Science Centre OX14 3DB, Abingdon, Oxfordshire, UK
- 17) Laboratorio Nacional de Fusión, Asociación EURATOM-CIEMAT, Madrid, Spain
- 18) Centro Ricerche Energia ENEA Frascati, Associazione Euratom-ENEA sulla Fusione, Frascati, Italy
- 19) Department of Physics, University of Wisconsin, Madison, WI, USA
- 20) Ass. Euratom/ENEA/CREATE, DIEL, Università di Napoli Federico II, Napoli, Italy
- 21) Universidad Carlos III de Madrid, Madrid, Spain
- 22) Ass. Euratom/ENEA/CREATE, DAEIMI, Università di Cassino, Cassino, Italy
- 23) Fusion for Energy Joint Undertaking, 08019 Barcelona, Spain (present address)

e-mail contact of main author: piero.martin@igi.cnr.it

Abstract. The paper summarizes the main achievements of the RFX fusion science program. RFX-mod is the largest reversed field pinch in the world, equipped with a very advanced system of 192 coils for active control of MHD stability. The discovery and understanding of helical states with electron internal transport barriers significantly advances the perspectives of the configuration. In the ITER era, the RFX program is also providing important results for the fusion community and in particular for Tokamak and Stellarator on feedback control of MHD stability and on three-dimensional physics

1. Executive summary: RFX mission, biennium highlights and open questions

1.1. Mission

The mission-oriented RFX fusion science program is shaped to provide a focused contribution to ITER and its accompanying fusion program. RFX-mod is a flexible reversed field pinch (RFP) toroidal device (major radius $R=2$ m and minor radius $a=0.46$ m) with plasma current 2 MA and volume 10 m^3 . As in all RFPs, plasma heating is purely ohmic; RFP could in principle obtain fusion power with ohmic heating only, and with magnetic field much smaller than in Tokamak – avoiding superconducting coils. RFX-mod is equipped with the best system of active coils for feedback control of plasma MHD stability: 192 coils, independently driven, cover the whole plasma surface.

The major challenges of RFP research, and of RFX-mod in particular, are: (a) rapidly advancing its performance, to assess the viability of the RFP approach to fusion; (b) providing state-of-the-art contribution to the global task of feedback control of MHD stability, with experiments done both in RFP and in tokamak configuration; (c) focusing on the key topic of three-dimensional magnetic shaping in a growing collaboration with the Stellarator community, (d) training new generation of fusion scientists, continuously being a strong and useful partner of ITER and of the fusion community

1.2. Highlights

Since the last Fusion Energy Conference in 2008 [1] the RFX-mod fusion science program has crossed several important milestones and is continuously progressing with profitable partnerships with Tokamak and Stellarator.

After extensive optimization of 1.5 MA regimes – where the improved performance of the self-organized spontaneous helical equilibrium with a single helical axis (SHAx) has been broadly documented [2] – the program focussed on the exploration of plasma currents toward *the maximum RFX-mod design value of 2 MA*. A number of technical improvements (including active cooling of the primary windings [3]) and the development of a new start-up

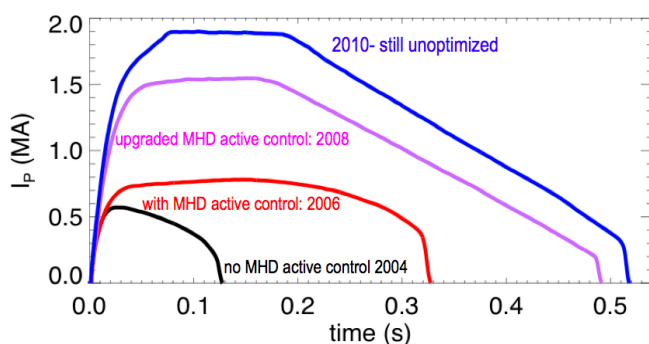


Figure 1: plasma current waveforms obtained in RFX-mod since its restart in December 2004

scenario [4]) allowed for physics exploration at plasma current $I_p \approx 1.8$ MA and for preliminary experiments at 2 MA. The latter, though far from being optimized, show no technical limit for operation at 2 MA and confirm the robustness of the device. Examples are shown in Figure 1.

Significant progress on understanding of SHAx state has been made. SHAx states have strong electron internal transport barriers (eITB) [5], where minimum electron

heat diffusivity $\chi_{e,\min} \approx 5\text{ m}^2\text{s}^{-1}$ is measured. This coincides with a region of null magnetic shear, as in tokamak, and of significant $\mathbf{E} \times \mathbf{B}$ sheared poloidal flow. The value of $\chi_{E,\min}$ expressed in Bohm units is consistent with data from similar Tokamak and Stellarator databases, confirming that in the barrier region RFP transport is approaching the quality of other configurations. The experimental particle transport coefficient in the helical core is reduced compared to the multiple helicity case, reaching values of the same order of magnitude of the volume averaged diffusivity estimated with a test particle approach in helical geometry. The $1/\nu$ transport regime (super-banana effects) typical of un-optimized Stellarator, is not found in numerical simulation [6]. Strong edge electron transport barriers

are also observed, though not necessarily linked with single helicity (SH) states. They lead to electron pressure pedestal, with $\nabla T_e \approx 80 \text{ keVm}^{-1}$. A suite of numerical codes has been assembled to study helical states, *in a strong partnership with the stellarator community* [6,7]. Helical eITBs appear at moderate density (Greenwald fraction $n/n_g \leq 0.25$), consistent with the evidence that the magnetic bifurcation leading to SHAx states occurs at low collisionality. Quasi Single Helicity (QSH) states are obtained up to $n/n_g \approx 0.35$, but without eITBs. Such density limit is attributed to localized edge density accumulation and plasma cooling, in combination with helical plasma wall interaction [8,9].

A rich program on active control of MHD stability has provided a large number of new results [10]. Real time control experiments have been performed operating RFX-mod both as RFP and as tokamak, to address control of resistive wall modes (RWM), tearing modes (TM) and magnetic field errors. Improvements are obtained by including in control models toroidal geometry and non-uniformity of the passive structures, and by taking into account the coupling between sensor and coils in MIMO models. Mode tracking experiments have been successfully used to apply a non-zero single helicity reference edge magnetic field, to sustain a single helical mode at desired edge amplitude. RWM non-rigidity was studied. Downgrading and reconfiguring the 192 active coils showed that the most unstable RWM can still be controlled by reducing the active coil coverage to 25% of the plasma surface. This was performed in collaboration with JT-60SA to help the design of its set of active coils. *A new integrated “flight-simulator” for closed loop control experiments was developed and benchmarked.*

RFX-mod can be run as a tokamak, with 120 kA plasma current lasting up to 1.2 s. In this configuration a current-driven (2,1) RWM is observed in ramped current plasmas as $q_{\text{edge}} \approx 2$. This mode is actively stabilized so that *for the first time a feedback stabilized $q_{\text{edge}} \approx 2$ tokamak plasma is run without disruptions.*

1.3. Open issues and future perspectives

The results obtained since last FEC proved the transformational nature of the helical RFP state. Nowadays RFX-mod routinely operates at high current in regimes of very low magnetic transport in the core, as a result of spontaneous self-organization. Two main open issues represent now the remaining challenges on confinement.

The first one concerns density control: at high current it is difficult to achieve helical states with high density. In general, high current, high density operation is prevented by high first wall recycling. This leads to edge peaked density profile and edge cooling, which makes the edge plasma highly resistive. This is a particularly critical issue since, if the edge is resistive, more input power is required to drive the poloidal current necessary to sustain the RFP configuration. Inherently associated to this is the second open issue, which deals with the ohmic input power that is still higher than expected, with a negative impact on the global energy confinement time. One reason for this is the edge density, as just explained, but other causes might be present, linked for example with a still un-optimized magnetic boundary. To improve density control, Hydrogen pellet fuelling is combined with wall-recycling control by means of lithization [8]. First tests with Lithium give better density control and more peaked profiles. Significant core density increase is obtained with H pellets.

In absence of “first-principle-based” show-stopper, most of the limits appear to be operational (e.g. first wall or active control optimization), and therefore solvable. Next steps in the RFX science program will address these difficult challenges relying on both a clear path and robust and flexible tools available to follow it. The path to exploitation of 2 MA RFX-mod with improved first wall conditioning and optimized magnetic boundary, supported by a growing effort on three-dimensional modelling, is open and worth being followed.

2. Optimization of high current operation

RFX-mod is in a unique position to test scaling of plasma performance with current and to

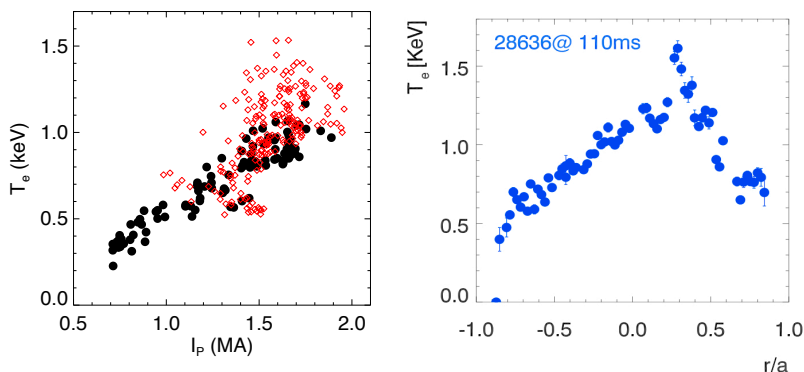


Figure 2. Left. core T_e vs. I_p for two different ranges of n/n_{gw} : [0.05,0.13] (red diamonds) and [0.14,0.21] (black circles). Each point is an average during I_p flattop. Right: typical high current electron temperature profile.

explore RFP physics in the MA range. Plasma current is a major control parameter for performance. Past experience, reported in the previous FEC, [1] indicated significant changes in RFX-mod plasma performance as plasma current was raised above 1 MA. The central electron temperature increase with I_p up to values ≥ 1.5

keV (see Figure 2) is confirmed by recent experiments up to $I_p \approx 1.8$ MA. Electron heating translates in increased magnetic Lundquist number S . The decrease of the amplitude of internally resonant tearing modes with increasing S was previously observed in MST [11] and confirmed by RFX-mod in a broader S range [1]. The novelty from RFX-mod is that the positive S -scaling of high n mode amplitudes (called secondary modes) is synergic with the dependence on S and plasma current of the innermost resonant mode amplitude ($m=1, n=-7$, the dominant mode). This is the background for the emergence at $I_p \geq 1.5$ MA of the helical SHAx states [1,2]. The growth of the dominant mode leads to core ordered helical topology, with a single helical axis. The decrease of secondary modes drives magnetic chaos reduction.

Producing high quality plasmas at high current, close to the machine design limit, calls for careful scenario design, which will be described in the following subsections.

2.1. High-current discharge setting-up

The 12 modular AC/DC converters that feed the toroidal and poloidal field circuits have recently been reconfigured to make more energy available for the magnetizing windings that drive the loop voltage: more energy is available to extend the initial current ramp and reach easily 2 MA and beyond. [4]. An example of this setting up is shown in Figure 1 for the highest I_p discharge.

2.2. Error field correction

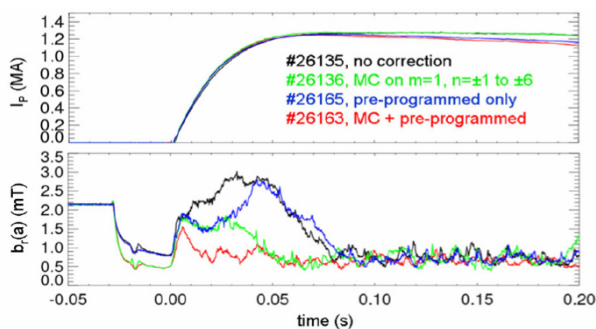


Figure 3: (top) current waveforms. (bottom) different error field control schemes. Mode control with feed-forward error control provides best correction (red curve)

In RFX-mod, during the current ramp-up phase, the vertical magnetic field penetrates faster through the two poloidal gaps in the shell and reproducible field errors of few mT are observed, toroidally localized at the gap positions. Reference signals recorded in dry runs are then used for active correction in feed-forward mode. Reference signals are computed with a dynamic decoupler [12] (described in Sect. 6), which uses the frequency

dependence of the coupling between actuators and sensors. Adding to the pre-programmed error control the feedback for the main modes contributing to the error field (i.e. $m=1$, $n=\pm 2$, $n=\pm 4$, $n=\pm 6$) a very good and robust correction is achieved (Figure 3) [10].

2.3. Gain optimization for tearing mode controller

Tearing modes are always present in RFPs, since they drive the dynamo magnetic self-organization process. Their amplitudes correspond to non-linear saturation and a k -spectrum that can be narrow or broad depending on the plasma regime (Single Helicity - SH or Multiple Helicity - MH). They cannot be fully suppressed and a feedback control system can at best zeroing the edge amplitudes of their radial components, $b_r(a)$. For this purpose optimized

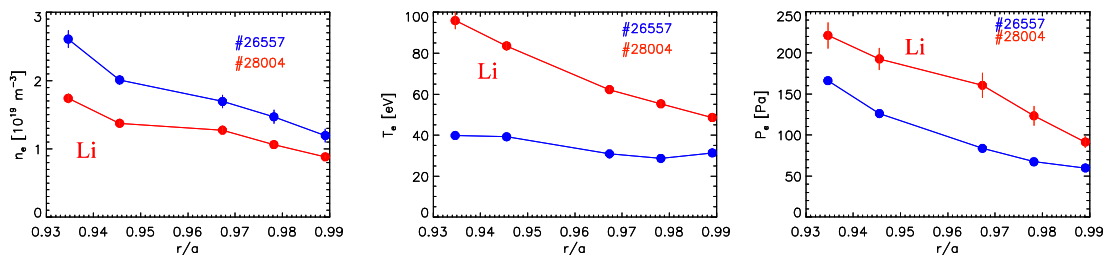


Figure 4: Edge density, temperature and pressure measured by Thermal Helium Beam diagnostic on similar discharges before #26557 and after lithization #28004.

gains for each individual active coil need to be used. The optimized proportional-integral-derivative (PID) gains leading to the smallest $b_r(a)$ have been calculated by an equilibrium model for a single tearing mode [13] - see Section 6-, and checked by an experimental scan.

2.4. Control of the first-wall properties and of density profiles

In order to reduce graphite first wall high recycling and improve control of the density profile, in particular at high current, first wall lithization has been tested besides boronization [8]. Experiments up to now have concentrated on injection of Li room temperature pellets (1.5

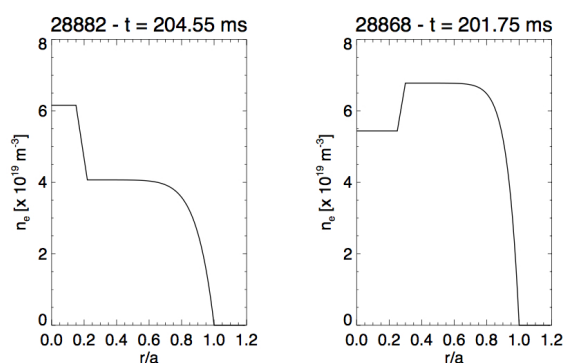


Figure 5: inverted density profiles with pellet ablation occurring inside (left) or outside (right) the barrier. Inversion is done assuming simplified model profiles

mm diameter, 6mm length) and only recently a Liquid Lithium Limiter, on loan from FTU [14] has been tested. Li pellet injection in a series of Helium discharges provides nearly uniform Li wall deposition. For each campaign a maximum of only 50 Li pellets were injected corresponding to 2×10^{22} atoms, ≈ 1 g, for a theoretical coating thickness of about 10 nm. Such rather low amount of Li, compared to the experience in the literature, is nonetheless effective in maintaining hydrogen wall recycling and impurity influx very low. After lithization edge temperature increases and electron density decreases; overall a higher edge pressure compared to discharges performed before Li wall conditioning is observed (Figure 4). Particle confinement time increases by 20%. Present experiments are promising and more intensive lithization is expected to produce stronger effects, extending to the core. H pellet injection is an effective way to refuel plasma core, in particular during SH states. Successful injection leads to core peaked density profiles in presence of internal transport barriers, as shown in Figure 5.

3. Helical states and internal transport barriers: evidence and understanding

RFX-mod plasmas at current ≥ 1 MA reproducibly show Quasi SH (QSH) states with ($m=1, n=-7$) helicity. Following the empirical scaling law already discussed in [1], their persistence increases up to $\approx 80-85\%$ at $I_p = 1.8$ MA. For $I_p \geq 1.5$ MA, QSH turns into SHAx. SHAx states are a necessary condition for electron internal electron transport barriers (eITB) [2,5]. eITB corresponds to steep electron temperature gradient (Figure 6), and to a minimum of the thermal conductivity. It also represents a region of reduced particle transport affecting both main gas and impurities.

The location of eITB foot coincides with a point of null shear in the safety factor q profile [6] (see Figure 7), which in the case of the RFP correspond to a q maximum. For Tokamak, where eITBs are also triggered by q reversed shear, a proposed interpretation is based on lower density of rational surfaces and thus on lower probability of mode coupling [15]. In

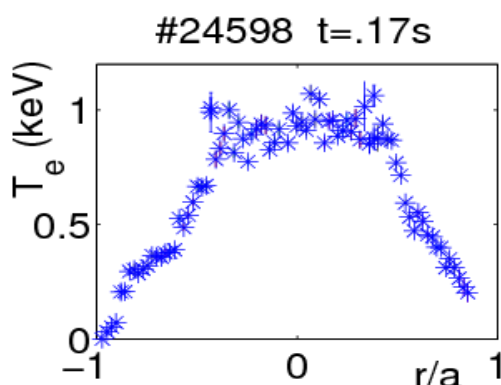


Figure 6: electron temperature profile with eITB

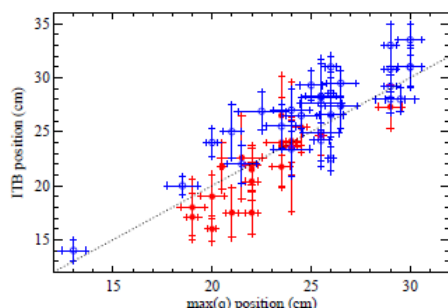


Figure 7: Position of the ITB vs the q maximum location for RFX-mod experimental DAx (full points) and SHAx states (empty points).

RFX-mod barriers are correlated also with flow shear. Non-linear three-dimensional (3D) MHD simulations show that the dynamo velocity field features a maximum in the shear profile, which occurs at the location q maximum [7]. Experimentally, the reconstruction of poloidal flow pattern [5] shows an inversion of the flow internal to the field reversal surface, indicating that flow shear is present, though spatial resolution does not allow discriminating whether higher shear corresponds exactly to maximum q . Edge flow shows (1,7) modulation consistent with magnetic topology [9].

In the experiment the ratio between the dominant and secondary modes increases as collisionality gets lower, a condition favoring SHAx (but resistivity may play a role, too). eITBs develop at low values of the collisionality, with $n/n_G \leq 0.25$. This limit is likely due to edge phenomena and in particular to helical plasma wall interaction (PWI) (Figure 8) [9]. The edge region in QSH is characterized by a chain of $m=0, n=7$ islands, arising as an effect of toroidicity and mode coupling [16]. These islands cause small helical shift and localized PWI, which determines edge localized density accumulation and plasma

cooling. Floating potential has helical modulation, interpreted as a modulation of electron fluxes towards the wall. These localized kinetic perturbations are supposed to facilitate the growth of secondary modes, opposing QSH. Even back-transitions to MH, observed during QSH states, are attributed to reconnection events [17] linked with helical PWI.

Pellet injection is used for refueling the helical core and creating a peaked density profile since the barrier is effective also for particles: it confines particles inside and prevents penetration from outside. Figure 5 shows two density profiles: on the left a case where ablation occurs in the centre, thus peaking the density; on the right a case where the pellet is ablated outside the barrier and the density profile remains hollow. A similar conclusion is inferred for impurities in experiments with Nickel Laser Blow Off and Neon puffing [5].

Experimental particle (H) diffusion coefficient D in the barrier is reduced by about one order-of-magnitude, with $D \leq 5 \text{ m}^2/\text{s}$, and negligible pinch velocity. The field line tracing code ORBIT [28] also indicates that in SHAx the diffusion coefficient at low collisionality is reduced by about two orders of magnitude with respect to the situation dominated by magnetic chaos, leading to $D \approx 0.5\text{-}5 \text{ m}^2/\text{s}$. This is lower but in the same range than the experimental evaluation. Electron heat diffusivity χ_e at the barrier decreases to minimum values $\chi_{e,\text{min}} \approx 5 \text{ m}^2/\text{s}$. It is worth noting that the value of χ_e expressed in Bohm units is consistent with similar databases obtained in Tokamak or Stellarator confirming that in the region of eITB the RFP is now approaching the transport quality of the other configurations. Both $\chi_{e,\text{min}}$ and the electron temperature gradient length L_{Te} scale inversely with the total amplitude of the secondary $m=1$ modes [5], indicating a strong link between the quality of magnetic topology, i.e. the level of magnetic chaos, and the strength of the barrier.

Preliminary evidence of a limit value for L_{Te} suggests the presence of other gradient-driven transport mechanisms emerging when magnetic chaos is reduced. Analytical work showed that ITG modes are more stable in RFPs than in Tokamaks because of stronger Landau damping [18]. Various numerical tools developed for tokamak turbulence studies have been adapted to RFP: the nonlinear electromagnetic (flux-tube) gyrokinetic code GS2 [19] and the full-radius fluid (ITG-TEM electrostatic turbulence) code TRB [20]. An integral eigenvalue approach, retaining full Finite-Larmor-Radius effects has also been used [7]. All agree that ITG modes hardly become linearly unstable in present experimental conditions. Trapped Electron Modes (TEM) could arise with density gradients stronger than those now measured.

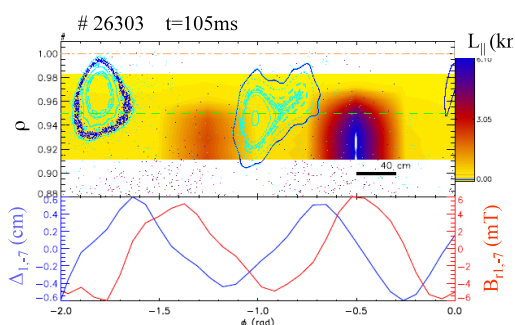


Figure 8: (up) Edge Poincaré plot ($\theta=0^\circ$) of (0,7) island chain and characteristic electron length L_{II} (color coded map); (down) toroidal behavior of the shift of dominant mode (blue) and of corresponding radial magnetic field (red).

Work to assess the impact of TEM on edge transport is on-going.

Gyrokinetic calculations show that a strong candidate to limit the temperature gradient is the micro-tearing (MT) instability that is the dominant micro-turbulence mechanism acting on the ion Larmor radius scale. MTs, driven by the electron temperature gradient, may lead to chains of overlapping magnetic islands and to local stochastization of magnetic field lines near mode rational surfaces. In the T_e gradient region MT modes are unstable [7]. Quasi-linear estimate of electron thermal conductivity related to MT falls in the range $\chi \approx 5 \div 20 \text{ m}^2/\text{s}$,

consistent with experimental values. eITBs correspond to better values of the energy confinement time ($\approx 5 \text{ ms}$ assuming $T_e=T_i$). Such values of the global confinement time are still not optimal due to the large power still required to sustain the poloidal current flowing in the relatively resistive edge plasma.

Signature of Global Alfvén Eigenmodes and Reversed Shear Alfvén Eigenmodes is experimentally detected at the plasma edge, though without significant impact on transport [21]. The physics of eITB in RFX-mod has several similarities with that in Tokamak and Stellarator. The most striking analogy is with the Tokamak, concerning the presence in both cases of a null in the q shear.

Analogies exist also with the Stellarator: for example the low collisionality and the presence of a significant flow shear. Both eITB and, as discussed later, the external transport barriers (ETB-see next section), are found so far in RFX-mod in regimes of low collisionality. Whether this analogy is a signature of a similar physics favoring the barrier is an open question. In Stellarators, low collisionality regime is related to the development of large

positive radial electric field E_r in the core, and consequently to shared flow (the electron root regime [22]). In RFX-mod, eITBs are strongly coupled to the onset of the SH equilibrium, which is also observed at low collisionality. Still an open question is whether, in the barrier region of the 3D SHAx topology, transport is described by neoclassical theory and if an ambipolar electric field shear builds up as in the Stellarator e-root regime.

4. Edge transport barriers

A new type of very strong electron transport barriers has been observed at the plasma edge ($r/a \approx 0.8$), where a pedestal up to 1 keV high develops in few cm [5]. In these conditions T_e gradients reach values up to 70-80 keV/m. An example is shown in Figure 9. These edge barriers correspond also to pressure barriers; however the dominant contribution derives from the temperature profile. ETBs do not necessarily require the presence of a SHAx state and typically appear at low density. Cases where both eITB and ETB coexist have been found.

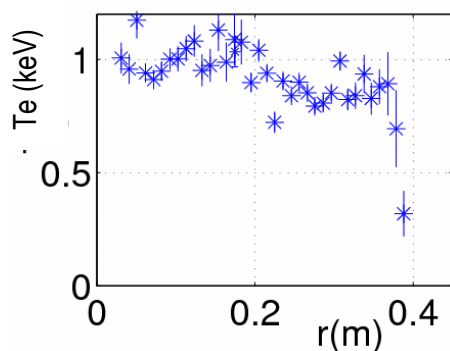


Figure 9: example of external transport barrier

ETB develop in regimes when secondary modes are relatively low, at low collisionality and prefer regimes with shallow edge toroidal magnetic field reversal. Magnetic chaos reduction appears to be a common feature of both internal and external barriers. ETB develop in fact in a region characterized by ordered magnetic surfaces, as shown by the field line tracing reconstructions made with the FLiT code [23]. The existence of a significant edge transport barrier expands the possibilities of operating improved confinement RFP regimes.

5. Building a three-dimensional knowledge

The discovery of Single Helical Axis States (SHAx) gives a unique opportunity to investigate the physics of three-dimensional (3D) fields in magnetized fusion plasmas and to broaden the knowledge basis in this area. There is, in fact, a growing interest both in the Stellarator and in the Tokamak community on the effects of 3D shaping of the magnetic field. The study of 3D RFX-mod features is benefiting of widely known codes originally developed for the Stellarator and adapted to the RFP in a growing collaborative effort.

Helical magnetic equilibrium is described analytically and numerically via both a perturbative analysis in toroidal geometry and a full 3D approach.

The analytical calculation [7] of ohmic RFP single helicity states is performed in the frame of resistive MHD in cylindrical geometry, by using perturbation theory for a paramagnetic pinch with low edge conductivity and axial magnetic field. A necessary criterion for toroidal field reversal at the edge is derived. The criterion involves the radial profile of the logarithmic derivative of the Newcomb eigenfunction of the pinch. It is suggestive that a finite edge radial magnetic field might be favourable for field reversal.

In the numerical perturbative approach, implemented in the SHEq code [6], the zero order toroidal force balance is solved together with Newcomb equation, which provides helical field components [6]. Full 3D calculation is performed with VMEC [24], adapted to RFP by using poloidal flux as magnetic surface label [6]. In fixed boundary runs the magnetic surfaces match the prediction of both field line tracing codes and the analytical approach. While the magnetic field topology is helical, $|\mathbf{B}|$ keeps an approximate axisymmetric shape. The RFP free-boundary version of VMEC, under development, will allow modelling an externally imposed magnetic field. Investigation on the use of externally applied rotational transform is under way [25]. SHEq 3D equilibria are used as input to ASTRA [26] code to interpret

experimental transport measurements. Preliminary analysis of ideal stability with Terpsichore code [27] indicates that symmetry breaking modes (1,8) and (2,15) are more stable with core reversed shear than with null shear.

3D fields also play an important role in determining transport. In SHAx, neoclassical effects, together with microturbulence, might have a significant role in ruling transport in the helical core and across internal barriers. Two main approaches for numerical study of transport in helical states are used. The first is based on the ORBIT code [28]: volume averaged particle transport coefficients across helical surfaces are estimated numerically by a mono-energetic test particle approach [29]. This approach takes into account both the drifts of particles

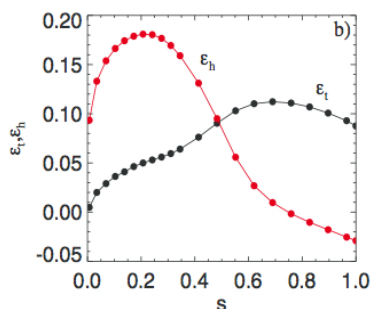


Figure 10: radial profile of the helical and toroidal ripple for a RFX-mod SHAx state

trajectories and the effect of the residual magnetic chaos. Work is in progress to implement in ORBIT also an electric field perpendicular to helical surfaces. A complementary approach is based on DKES [30], in order to estimate the full matrix of local neoclassical transport coefficients. This is based on the assumption that transport is described by a local approach.

As done in Stellarators deviations from axi-symmetry are described by means of the radial functions $\epsilon_h(s)$ and $\epsilon_t(s)$, the helical and the toroidal ripple respectively [6]. As shown in Figure 10, ϵ_h is dominant in the central region ($\epsilon_h \approx 2-3 \epsilon_t$) and ≈ 0 at the edge ($\epsilon_h \approx 0.1-0.2 \epsilon_t$). Thus, while the core is strongly helically deformed, the outer

region almost preserves typical properties of a quasi-axisymmetric configuration. Neoclassical effects, and in particular super-bananas, which affects un-optimized Stellarators at low collisionality, might not be a significant issue. ORBIT shows that when trapped particles drift out of the helical core with high ϵ_h , they reach a region ($r/a \approx 0.6$) where ϵ_h decreases. They become almost passing without being lost, at least at low collisionality. ORBIT MonteCarlo simulations confirm that ion diffusion coefficient (D_i) - volume-averaged over the helical domain – plotted vs. collisionality ν does not show the $1/\nu$ regime typical of

un-optimized Stellarators (Figure 11).

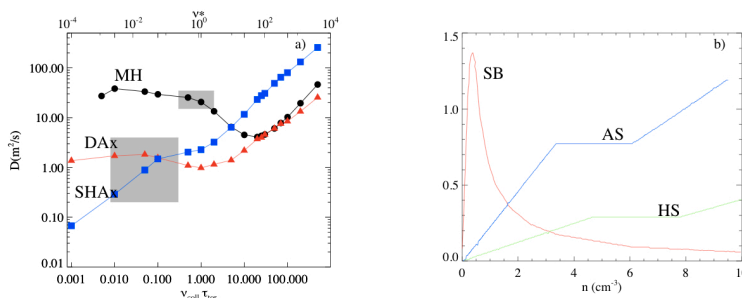


Figure 11. Left: Diffusion coefficient D of H^+ ions as a function of $\nu_{\text{coll}} \tau_{\text{tor}}$ (black=MH, red=QSH, blue=SHAx). Right: schematic view of the neoclassical transport regimes: AS=axisymmetric system, HS=helically symmetric, SB = superbanana (adapted from H. E. Mynick, Phys. Plasmas **13**, 058102, (2006).

The addition of self-consistent heat transport dynamics to three-dimensional non-linear MHD codes is expected to provide significant improvements in modeling of RFP self-organization [7]. To this end the PIXIE3D initial value code has been

implemented for RFP. Recently, careful benchmarking against the SpeCyl code has successfully completed the mandatory step of numerical verification.

6. Active control of MHD stability

Research on feedback control of MHD stability is providing key results [10]. Real time control experiments have been performed operating RFX-mod both as RFP and as tokamak, to address resistive wall modes (RWM), tearing modes (TM) and error field control.

Improvements are obtained by including in control models toroidal geometry and deviations from uniformity of passive structures. A first technique is based on a stationary decoupling matrix, which is effective in producing pure harmonics at the sensor radius. The dynamical pseudo-decoupler is a more elaborated tool, which takes into account the frequency dependence of the toroidal (poloidal) coupling. As previously shown (Section 2), its use substantially decreases time varying toroidally localized field errors in the start-up phase.

3D features of the magnetic boundary, like gaps in the resistive wall and portholes, influence RWM growth rates and spatial structure. Many poloidal harmonics contribute to the mode structure, even in the case of circular plasma like that of RFX-mod. Mode non-rigidity has been studied. The 192 active coils set can be on purpose downgraded and reconfigured, to test

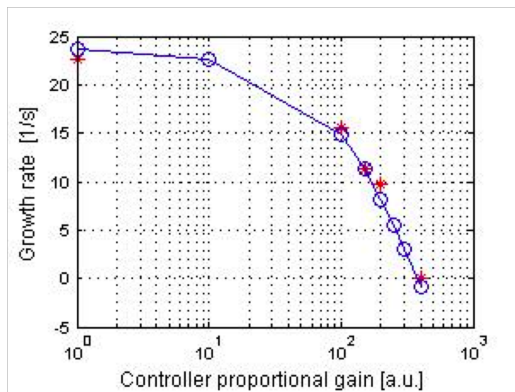


Figure 12: Numerical growth rates computed as a function of the controller gain (continuous curve-open dots) compared with experimental ones measured with high accuracy under the same controller conditions, i.e. using the same gains (asterisks) [34,]

the role of coil geometry and number on stabilization. This is done in collaboration with JT-60SA to help the design of its set of active coils [31]; the most unstable RWM can still be controlled by reducing up to 1/24 the active coil number (surface covered by coils down to 4.2%) after tuning of the gains.

RFX-mod is an excellent tool to benchmark against experimental data complex numerical codes used to predict plasma stability and to simulate the behaviour of real-time controllers. Accurate modelling of MHD stability and control is indeed a key request for ITER. This requires understanding the effects on stability of plasma rotation and of the complex 3-d conducting structures

surrounding the plasma. Since RWM stability in RFP is not affected by dissipation and flow [10], RWM modelling can focus on 3D effects removing other sources of uncertainties. A 3D model of RFX-mod has been implemented in the code CarMa and benchmarked against RFX-mod RWM experimental data [32]. A cylindrical MHD model including plasma pressure and longitudinal flow has also been benchmarked against RFX-mod data [33].

A new integrated simulator for closed loop control experiments has been developed and benchmarked [34]. The tool couples self-consistently a full 3D description of the machine boundary (Cariddi code), a 2D toroidal model of stability (MARS) and a dynamic model of the control system cast in the state variable representation. Using actual PID gains and plasma equilibrium parameters such “flight simulator” successfully reproduces experimental closed loop RWM growth rates, as shown in Figure 12.

Control of resonant tearing modes is more challenging. Several TM are linearly unstable in the RFP, and nonlinearly reach saturated amplitude. Their dynamics under feedback control conditions is highly nonlinear: the increase of proportional gain reduces the edge radial field to a minimum; any further increase induces mode rotation. Since last FEC an intense activity to optimize feedback laws for resonant modes has been undertaken. Basic effects of the clean mode control (CMC) are explained in [13] using an equilibrium model for a single tearing mode. The model assumes the multiple shells structures of RFX-mod and is based on the balance between the electromagnetic torque - produced by the conductive structures and the feedback coils surrounding the plasma - and the viscous torque due to the fluid motion. Recently the model has been upgraded and now a more accurate diffusion equation, which takes into account the shell thickness, is used to describe the shell penetration [13]. More complete multimode dynamic model, implemented in the RFXlocking code [13] is also

developed. This model evolves the mode frequencies and edge amplitudes of several tearing modes at the same time, taking into account not only the interaction with the external structures but also the non-linear interaction between themselves. The model has driven the experimental PID gain optimization previously discussed.

7. Tokamak operation in RFX-mod

Thanks to its high flexibility, RFX-mod can be run as a tokamak, with 120 kA plasma current and discharge duration up to 1.2 s. Plasma current is basically limited by the available toroidal field, which is not very large since the coils were designed with the RFP target.

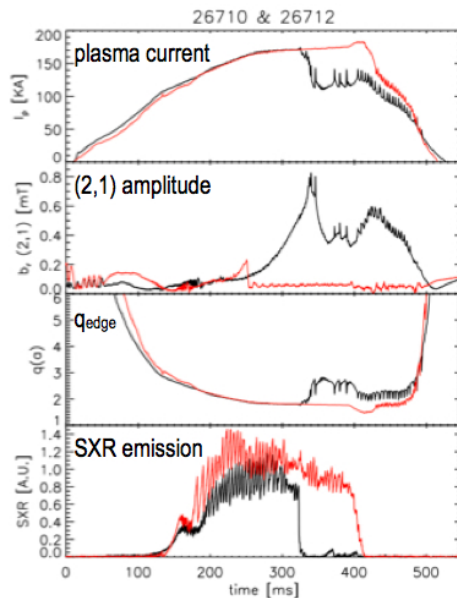


Figure 13: example of RFX-mod ramped current tokamak operation. Black curves: without feedback; growth of (2,1) evident. Red curves: with feedback; mode is kept at very low value

Tokamak plasmas were used to study edge turbulence with the same tools used in the RFP. More recently a project has started to use RFX-mod tokamak plasmas as test-bed for real time MHD active stability control. Even if RFX-mod tokamak has low current, it shares with larger device several MHD instabilities, which need to be controlled, and has the unique feature of a high performance system of active coils. In this configuration a current-driven (2,1) RWM is observed in ramped current plasmas as $q_{\text{edge}} \approx 2$ (q_{edge} is reconstructed from external measurements). The experiment follows an idea proposed for DIII-D [35,36] and HBT-EP [37] to excite current-drive external kink modes and then implemented in RFX-mod. Feedback control allows full stabilization of this mode, and for the first time a feedback stabilized

$q_{\text{edge}} \approx 2$ tokamak plasma is run without disruptions (Figure 13).

8. Conclusions

Since December 2004, when experiments started in the RFX-mod device, the RFX fusion science program has successfully reached a number of key milestones. New and transformational results have been obtained: they contribute to both RFP fusion physics and to advancement of fusion in general. RFX-mod is in fact proceeding in a strong partnership with Tokamak and Stellarator, and with full integration in the fusion program of the ITER era. A number of issues remain to be solved in the RFX-mod route for a full assessment of the RFP fusion potential. First wall behavior – in particular in terms of recycling -, and in general control of density profiles in helical states, need to be optimized. This will help both in enhancing plasma thermal content and in avoiding cool and resistive edge plasma, a feature that has a significant cost in term of input power. Further optimization of the quality of the magnetic boundary will also be helpful to reduce edge magnetic turbulence and magnetic driven transport, and to make more robust the helical states. Improvements on these two issues may lead to stronger and more reproducible edge pressure pedestal, an important requirement for a global improvement of confinement. More long-range activities, on current drive (experiments on Oscillating Field Current Drive started in RFX-mod), on tools for edge lost particle disposal and on optimization of the feedback system are going on. The device flexibility helps in testing proof of principle solutions.

Confidence on the path for the solution of these issues is given by the rich set of results obtained since 2004, and partially reported in this paper. The discovery of self-organized

helical states with electron internal transport barriers, and the achievement of core electron temperature ≥ 1.5 keV is a demonstration that RFP is not necessarily plagued by high magnetic transport. Active control of MHD stability proves that a thick shell is not necessary, and provides a very flexible tool to explore a number of ITER relevant questions. Unique in the fusion arena, RFX-mod can operate with active control both in Tokamak and RFP configurations. A growing subject like that of three-dimensional fusion physics has RFX-mod as an active player, with strong integration with Stellarator and Tokamak communities. RFX-mod has also supported the community with new contributions to key topics like density limit of turbulence driven transport. The completion of on-going diagnostic projects and the installation of a 1 MW, 25kV H beam, on loan from AIST Tsukuba, will enhance the portfolio of tools for exploring RFP physics also on new topics, like fast ions.

RFX-mod is in an excellent position to taking up the challenge of setting a milestone in the route for the assessment of RFP potential as an ohmic, low-magnetic field, high engineering beta fusion reactor

Acknowledgments: the authors wish to thank the whole technical and administrative staff of Consorzio RFX for the continuous and generous support.

-
- [1] MARTIN P. et al., Nucl. Fusion, **49**; 104019 (2009)
 - [2] LORENZINI, R. et al. Nat. Phys. **5**, 570 (2009)
 - [3] FANTINI, F. et al., “New cooling system with dielectric fluid for magnetizing winding in RFX-mod experiment”, presented at the 26th SOFT Conference, 2010
 - [4] ZANOTTO, L et al., in Proc. 37th EPS conference on plasma physics, paper P2.193 (2010)
 - [5] PUIATTI, M.E. et al. “Internal and edge electron transport barriers in the RFX-mod Reversed Field Pinch”, paper EXC/P4-10, this conference (2010)
 - [6] MARRELLI, L. et al, “Three-dimensional physics studies in RFX-mod”, paper EXS/P5-10, this conference (2010)
 - [7] CAPPELLO S., et al., “Equilibrium and Transport for Quasi Helical Reversed Field Pinches”, paper THC/P4-03, this conference (2010)
 - [8] DAL BELLO, S. et al., “Lithisation effects on density control and plasma performance in RFX-mod experiment”, paper EXD/P3-06, this conference (2010)
 - [9] SCARIN, P. et al “Magnetic structures and pressure profiles in the plasma boundary of RFX-mod: high current and density limit in helical regimes”, paper EXD/P3-29, this conference (2010)
 - [10] BOLZONELLA, T. et al, “Advanced Control of MHD Instabilities in RFX-mod”, EXS/P5-01, this conference (2010)
 - [11] STONEKING M.R., et al. Phys. Plasmas **5** 1004 (1998)
 - [12] SOPPELSA et al., Fusion Eng. Des. **83** 224-227 (2008)
 - [13] ZANCA P., Plasma Phys. Control. Fusion **51** 015006 (2009)
 - [14] APICELLA, M.L., et al., Journal of Nuclear Materials **363–365**, (2007) 1346
 - [15] GARBET X. et al, Phys. Plasmas **8**, 2793 (2001)
 - [16] SPIZZO, G. et al., Phys. Rev. Letters **96** 025001 (2006)
 - [17] ZUIN M. et al, Plasma Phys. Control. Fusion **51** 035012 (2009)
 - [18] GUO S C, Physics of Plasmas **15** 122510 (2008)
 - [19] PREDEBON I., et al. Phys. Plasmas **17** 012304 (2010)
 - [20] F. SATTIN, et al Plasma Phys. Control. Fusion **52**, 105002 (2010)
 - [21] SPAGNOLO, S. et al., Proc. 37th EPS Conf. on Plasma Phys., paper P4.162 (2010)
 - [22] TAKEIRI Y et al., Phys. Plasmas **10** 1788 (2003)
 - [23] INNOCENTE P et al 2007 Nucl. Fusion 47 1092
 - [24] HIRSHMAN, S.P. and Whitson, J.C., Phys. Fluids **26** 3554 (1983)
 - [25] BOOZER, A.B and POMPHREY, N, Phys. Plasmas **16**, 022507 (2009).
 - [26] PEREVERZEV G et al., Rep. IPP 5/98, Garching, February 2002)
 - [27] COOPER W.A. et al., Fusion Sci. Technol. **50**, 245 (2006)
 - [28] WHITE R B, CHANCE M S, Phys. Fluids **27**, 2455 (1984)
 - [29] GOBBIN M., et al. Plas. Phys. Contr. Fus. **51** (2009) 065010
 - [30] HIRSMAN S.P. et al., Phys. Fluids **29** (1986) 2951
 - [31] TAKECHI M. et al, Proc. 37th EPS Conf. on Plasma Phys., Sofia 29/06-03/07/2009, **34E**, P-2.192 (2010).
 - [32] VILLONE F. et al., Phys. Rev. Lett. **100**, 255005 (2008)
 - [33] WANG Z.R. et al., Phys. Plasmas **17**, 052501 (2010)
 - [34] MARCHIORI G et al., in Proc. 37th EPS Conf. on Plasma Phys., paper P2.183 (2010)
 - [35] IN Y., et al, Nucl. Fusion **50** 042001 (2010) and IN Y., et al, Plasma Phys. Control. Fusion **52** 104004 (2010)
 - [36] OKABAYASHI, M. et al., Nucl. Fusion **49** 125003 (2009)
 - [37] CATES C., et al., Phys. Plasmas **7**) 3133 (2000)